

Measurement of the neutron capture cross section of the fissile isotope ^{235}U with the CERN n_TOF Total Absorption Calorimeter and a fission tagging based on micromegas detectors

E. Mendoza¹, J. Balibrea¹, D. Cano-Ott¹, C. Guerrero², E. Berthoumieux³, S. Altstadt⁴, J. Andrzejewski⁵, L. Audouin⁶, M. Barbagallo⁷, V. Bécaries¹, F. Bečvář⁸, F. Belloni^{3,2}, C. J. Billowes⁹, V. Boccone², D. Bosnar¹⁰, M. Brugger², M. Calviani², F. Calviño¹¹, C. Carrapiço¹², F. Cerutti², E. Chiaveri^{3,2}, M. Chin², N. Colonna⁷, G. Cortés¹¹, M.A. Cortés-Giraldo¹³, M. Diakaki¹⁴, C. Domingo-Pardo¹⁵, I. Duran¹⁶, R. Dressler¹⁷, N. Dzysiuk¹⁸, C. Eleftheriadis¹⁹, A. Ferrari², K. Fraval³, S. Ganesan², A.R. García¹, G. Giubrone¹⁵, M.B. Gómez-Hornillos¹¹, I.F. Gonçalves¹², E. González-Romero¹, E. Griesmayer²¹, F. Gunsing³, P. Gurusamy²⁰, D.G. Jenkins²², E. Jericha²¹, Y. Kadi², F. Käppeler²³, D. Karadimos¹⁴, T. Kawano²⁴, N. Kivel¹⁷, P. Koehler²⁵, M. Kokkoris¹⁴, G. Korschinek²⁶, M. Krtička⁸, J. Kroll⁸, C. Langer⁴, C. Lampoudis³, E. Leal-Cidoncha¹⁶, C. Lederer^{27,4}, H. Leeb²¹, L.S. Leong⁶, R. Losito², A. Manousos¹⁹, J. Marganiec⁵, T. Martínez¹, P.F. Mastinu¹⁸, M. Mastromarco⁷, C. Massimi²⁸, M. Meaze⁷, A. Mengoni²⁹, P.M. Milazzo³⁰, F. Mingrone²⁸, M. Mirea³¹, W. Mondelaers³², C. Paradela¹⁶, A. Pavlik²⁷, J. Perkowski⁵, M. Pignatari³³, A. Plompen³², J. Praena¹³, J.M. Quesada¹³, T. Rauscher³³, R. Reifarh⁴, A. Riego¹¹, F. Roman^{2,31}, C. Rubbia^{2,34}, R. Sarmiento¹², P. Schillebeeckx³², S. Schmidt⁴, D. Schumann¹⁷, I. Stetcu²⁴, M. Sabaté¹³, G. Tagliente⁷, J.L. Tain¹⁵, D. Tarrío¹⁶, L. Tassan-Got⁶, A. Tsinganis², S. Valenta⁸, G. Vannini²⁸, V. Variale⁷, P. Vaz¹², A. Ventura²⁹, R. Versaci², M.J. Vermeulen²², V. Vlachoudis², R. Vlastou¹⁴, A. Wallner²⁷, T. Ware⁹, M. Weigand⁴, C. Weiß²¹, T.J. Wright⁹, P. Žugec¹⁰

¹Centro de Investigaciones Energeticas Medioambientales y Tecnológicas (CIEMAT), Madrid, Spain

²European Organization for Nuclear Research (CERN), Geneva, Switzerland

³Commissariat à l'Énergie Atomique (CEA) Saclay - Irfu, Gif-sur-Yvette, France

⁴Johann-Wolfgang-Goethe Universität, Frankfurt, Germany

⁵Uniwersytet Łódzki, Lodz, Poland

⁶Centre National de la Recherche Scientifique/IN2P3 - IPN, Orsay, France

⁷Istituto Nazionale di Fisica Nucleare, Bari, Italy

⁸Charles University, Prague, Czech Republic

⁹University of Manchester, Oxford Road, Manchester, UK

¹⁰Department of Physics, Faculty of Science, University of Zagreb, Croatia

¹¹Universitat Politècnica de Catalunya, Barcelona, Spain

¹²Instituto Tecnológico e Nuclear, Instituto Superior Técnico, Universidade Técnica de Lisboa, Lisboa, Portugal

¹³Universidad de Sevilla, Spain

¹⁴National Technical University of Athens (NTUA), Greece

¹⁵Instituto de Física Corpuscular, CSIC-Universidad de Valencia, Spain

¹⁶Universidade de Santiago de Compostela, Spain

¹⁷Paul Scherrer Institut, Villigen PSI, Switzerland

¹⁸Istituto Nazionale di Fisica Nucleare, Laboratori Nazionali di Legnaro, Italy

¹⁹Aristotle University of Thessaloniki, Thessaloniki, Greece

²⁰Bhabha Atomic Research Centre (BARC), Mumbai, India

²¹Atominstut, Technische Universität Wien, Austria

²²University of York, Heslington, York, UK

²³Karlsruhe Institute of Technology, Campus Nord, Institut für Kernphysik, Karlsruhe, Germany

²⁴Los Alamos National Laboratory, Los Alamos, New Mexico 87545, USA

²⁵Oak Ridge National Laboratory (ORNL), Oak Ridge, TN 37831, USA

²⁶Technical University of Munich, Munich, Germany

²⁷University of Vienna, Faculty of Physics, Vienna, Austria

²⁸Dipartimento di Fisica, Università di Bologna, and Sezione INFN di Bologna, Italy

²⁹Agenzia nazionale per le nuove tecnologie, l'energia e lo sviluppo economico sostenibile (ENEA), Bologna, Italy

³⁰Istituto Nazionale di Fisica Nucleare, Trieste, Italy

³¹Horia Hulubei National Institute of Physics and Nuclear Engineering - IFIN HH, Bucharest - Magurele, Romania

³²European Commission JRC, Institute for Reference Materials and Measurements, Retieseweg 111, B-2440 Geel, Belgium

³³Department of Physics and Astronomy - University of Basel, Basel, Switzerland

³⁴Laboratori Nazionali del Gran Sasso dell'INFN, Assergi (AQ), Italy

Abstract

Actual and future nuclear technologies require more accurate nuclear data on the (n,γ) cross sections and α -ratios of fissile isotopes. Their measurement presents several difficulties, mainly related to the strong fission γ -ray background competing with the weaker γ -ray cascades used as the experimental signature of the (n,γ) process. A specific setup has been used at the CERN n_TOF facility in 2012 for the measurement of the (n,γ) cross section and α -ratios of fissile isotopes and used for the case of the ^{235}U isotope. The setup consists in a set of micromegas fission detectors surrounding ^{235}U samples and placed inside the segmented BaF_2 Total Absorption Calorimeter.

1 Introduction

Nuclear data on neutron-induced capture and fission cross-sections are necessary for improving the design and performance of advanced nuclear reactors and transmutation devices for the incineration of radioactive nuclear waste [1, 2]. The actual nuclear data priorities are summarized in the High Priority Request List [3] of the Nuclear Energy Agency, where the capture cross sections of four fissile isotopes has been included: $^{233,235}\text{U}$ and $^{239,241}\text{Pu}$. The difficulty of these measurements is that the detection of the capture reactions is performed by detecting the capture γ -rays, which in this case competes with the fission γ -ray background.

We have measured the $^{235}\text{U}(n,\gamma)$ cross section at the n_TOF facility [4, 5] with the Total Absorption Calorimeter (TAC) [6] and fission micromegas detectors (FTMGAS) [7]. Here we describe the experimental setup used and the first preliminary results.

2 The experimental setup

The CERN n_TOF neutron time-of-flight (TOF) facility delivers a neutron beam generated in spallation reactions induced by a 20 GeV/c pulsed proton beam of $7 \cdot 10^{12}$ protons per pulse and with 16 ns FWHM time resolution. The spallation target is a cylindrical lead block with 60 cm diameter and 40 cm length. The neutrons are moderated in a 4 cm thick borated water layer before traveling 185 m in vacuum until reaching the experimental area, where the measured samples and the detectors are placed.

We used 10 isotopically enriched samples of $^{235}\text{U}_3\text{O}_8$ produced at IRMM Geel. They have around $300 \mu\text{g}/\text{cm}^2$ surface density, and are deposited on 20 μm thick aluminum backings. They have a diameter of 42 mm, thus covering the entire neutron beam profile.

The (n,γ) reactions were measured with the Total Absorption Calorimeter, which is a segmented array composed by 40 BaF_2 crystals of 15 cm in length and covering 95% of the 4π solid angle. This detector is used to measure neutron capture cross sections by detecting in coincidence (nearly) all the γ -rays forming the cascades de-exciting the compound nucleus after the neutron capture reactions. The

fission reactions were measured with micromegas detectors, operated with a gas mixture of Ar 88%, CF₄ 10% and isobutane 2% at 1 atm. All the signals induced in the TAC and in the FTMGAS detectors were recorded by high-performance digitizers (Acqiris-DC270) with 8 bits resolution, operated at 250 MSamples/s and recording for each neutron pulse 32 ms long data buffers which contain the entire digitized electronic response of each individual detector [8].

The measurement was performed with the samples and the FTMGAS placed in the center of the TAC, surrounded by a 5 cm thick spherical neutron absorber shell made of borated polyethylene, used to reduce the background of scattered neutrons. This setup can be seen in Fig. 1. Two different fission configurations were used, based on 2 and 10 fission tagging micromegas detectors.

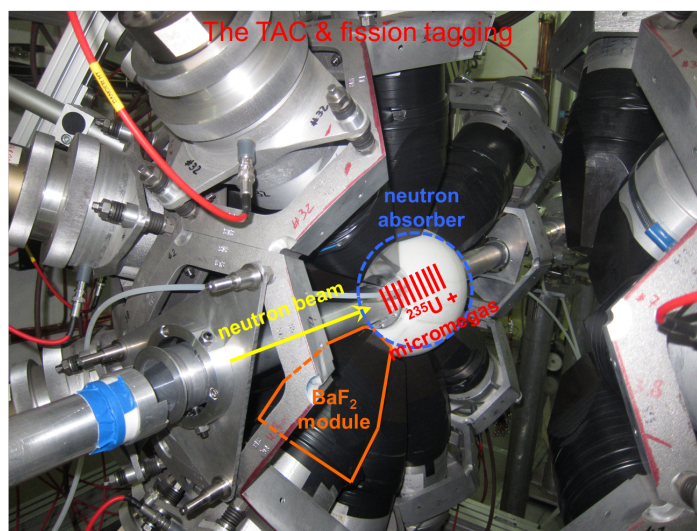


Fig. 1: Experimental setup of the $^{235}\text{U}(n,\gamma)$ cross section measurement. The ^{235}U samples and the FTMGAS are placed in the center of the TAC, which appears opened in two semispheres in the picture, surrounded by a neutron absorber.

The configuration with the 2 FTMGAS was dedicated to the $^{235}\text{U}(n,\gamma)$ cross section measurement. A stack of 8 bare ^{235}U samples and two samples encapsulated inside the FTMGAS were placed in the beam for improving the signal to background ratio (i.e. to minimize the amount of dead material from the fission tagging setup in the neutron beam). A low fission tagging efficiency of $\sim 20\%$ was achieved. As it has been demonstrated in [9], it is possible to remove accurately the gated fission γ -ray background at low tagging efficiencies by selecting events with a high γ -ray multiplicity which correspond only to (n,f) γ -rays and for which the TAC has a nearly 100% detection efficiency. Indeed, a simplified version of this technique, without any fission tagging, has been used as well at LANL in a ^{235}U cross section measurement [10]. The option of having fission tagging capabilities at a low efficiency has been preferred for the measurement at n_TOF for deducing the normalization of the data strictly from experimental parameters, without the need of a using evaluated cross section data as an external reference.

The configuration with the 10 FTMGAS was dedicated the $^{235}\text{U}(n,f)/^{235}\text{U}(n,\gamma)$ ratio (α -ratio) for well resolved resonances, as a cross check for the 2 FTMGAS data and for the measurement of γ -ray energy distributions from the lowest lying resonances. Each sample was inserted in a FTMG for measuring the fission cross section with a high efficiency ($\sim 90\%$) at the price of having a much larger dead material (i.e. background) than with the 2 FTMGAS configuration.

In both cases, dedicated background measurements with the same experimental setup but without the ^{235}U layers were performed, including all the dead material layers intercepting the neutron beam. Additional measurements with a ^{197}Au sample (capture cross section reference) and a carbon scatterer foil (for determining the neutron sensitivity) were also performed.

3 Preliminary analysis

The TAC measures in coincidence the γ -rays emitted after the capture reactions. The individual signals are grouped into TAC events, using a time coincidence window of 20 ns. Each TAC event is characterized by its time-of-flight, the total energy deposited (E_{sum}) and the crystal multiplicity (m_{cr}), which is the number of detectors contributing to the event above a given threshold. Conditions are applied to the detected events in E_{sum} and m_{cr} in order to improve the capture signal over background ratio. A coincidence analysis is also performed between the fission events detected by the FTMGAS and the TAC events. If a TAC event is in coincidence with a FTMGAS event, it is tagged as a fission event. The tagging efficiency can be calculated from the ratio of counts in the TAC in coincidence with the micromegas to the total number of counts in the TAC, for very restrictive conditions in the TAC events (high E_{sum} and high m_{cr}) which guarantee that the TAC event is a fission event. The preliminary values obtained for the tagging efficiency are 19.4(4)% and 90.0(3)%, for the 2 FTMGAS and the 10 FTMGAS configurations, respectively.

Examples of deposited energy spectra in the TAC are presented in Fig. 2, where two different backgrounds are presented. The one in blue (“Background”) has been obtained from the dedicated background measurements (dummy assemblies and measurements without beam), and does not include the background due to fission reactions in ^{235}U . The one in magenta (“Fission”) is the background due to fission in ^{235}U , and it has been obtained from the tagged events scaled by the inverse of the tagging efficiency.

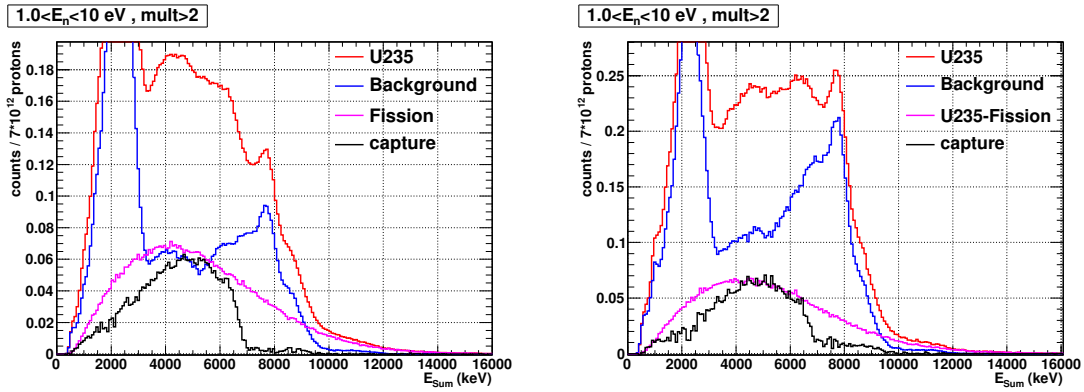


Fig. 2: Deposited energy spectra in the TAC corresponding to the $^{235}\text{U}(n,\gamma)$ measurement (red), the background excluding fission (blue), the fission events (magenta), and the capture events (black). All the spectra correspond to TAC events with $m_{cr} > 2$, and neutron energies between 1 and 10 eV. The results corresponding to the 2 FTMGAS configuration are presented in the left panel and the results corresponding to the 10 FTMGAS configuration in the right panel.

A preliminary experimental capture ($x = \gamma$) and fission ($x = f$) cross-sections have been calculated for each configuration with:

$$\sigma_{(n,x)} = \frac{1}{n_{at}} \frac{C_x(E_n) - B_x(E_n)}{\epsilon_x \cdot \Phi(E_n)}. \quad (1)$$

where C_x , B_x , and ϵ_x are the counting rate, background and detection efficiency of the TAC and the micromegas, respectively, and $\Phi(E_n)$ is the neutron energy fluence distribution.

A (very preliminary) cross sections have been obtained in this way, and are presented in Fig. 3 to Fig. 8. They have been normalized to the cross sections available in the ENDF/B-VII.0 library [11] in the 0.2-10 eV neutron energy range

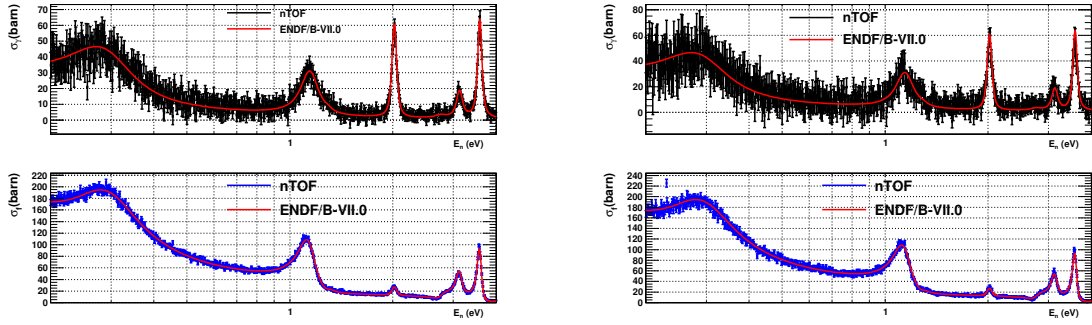


Fig. 3: Preliminary capture (top) and fission (bottom) cross sections obtained with the TAC and with the micro-megas, calculated from the 2 FTMGAS (left) and 10 FTMGAS (right) configurations, in the 0.2-4 eV energy range.

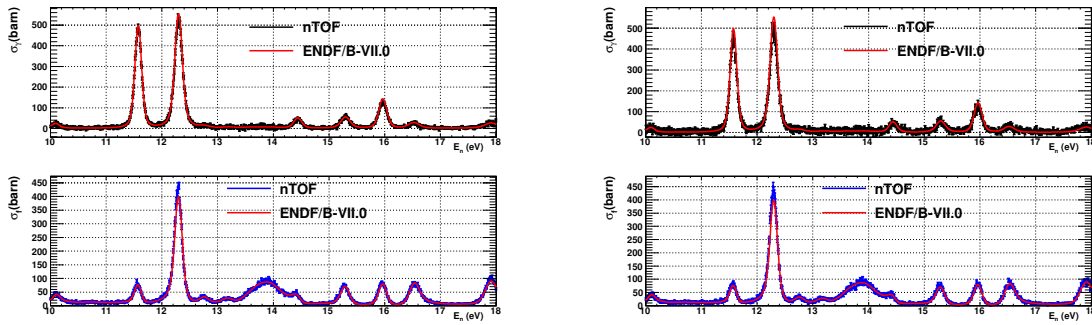


Fig. 4: Preliminary capture (top) and fission (bottom) cross sections obtained with the TAC and with the micro-megas, calculated from the 2 FTMGAS (left) and 10 FTMGAS (right) configurations, in the 10-18 eV energy range.

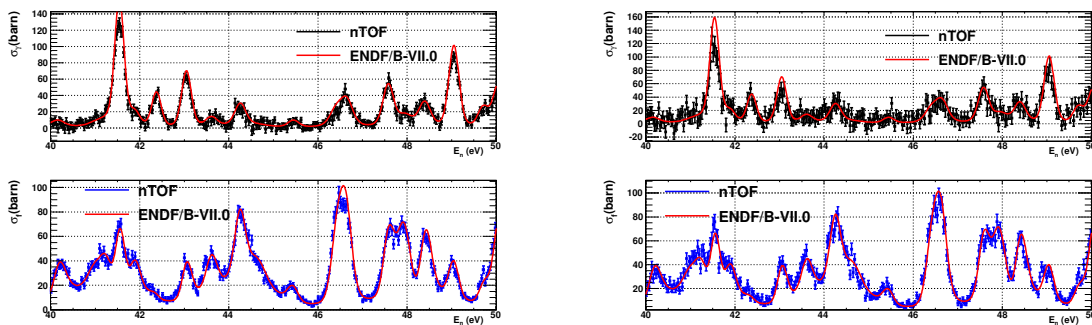


Fig. 5: Preliminary capture (top) and fission (bottom) cross sections obtained with the TAC and with the micro-megas, calculated from the 2 FTMGAS (left) and 10 FTMGAS (right) configurations, in the 40-50 eV energy range.

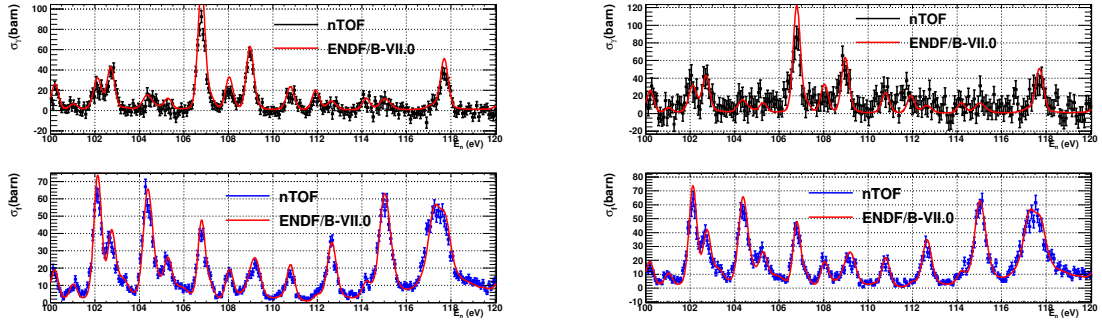


Fig. 6: Preliminary capture (top) and fission (bottom) cross sections obtained with the TAC and with the micro-megas, calculated from the 2 FTMGAS (left) and 10 FTMGAS (right) configurations, in the 100-120 eV energy range.

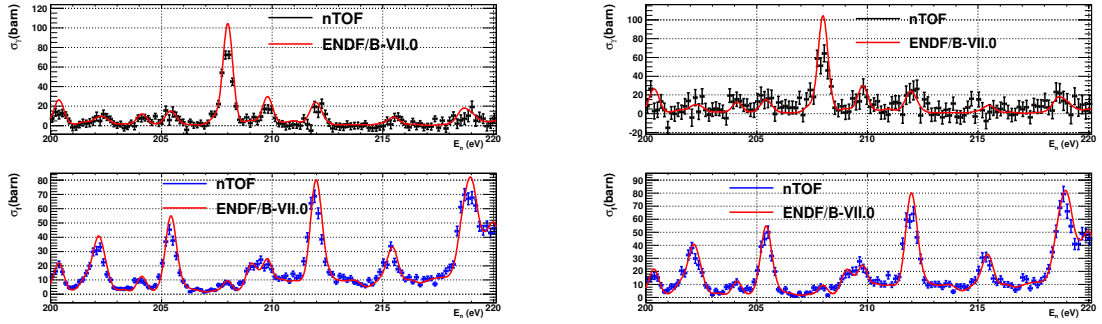


Fig. 7: Preliminary capture (top) and fission (bottom) cross sections obtained with the TAC and with the micro-megas, calculated from the 2 FTMGAS (left) and 10 FTMGAS (right) configurations, in the 200-220 eV energy range.

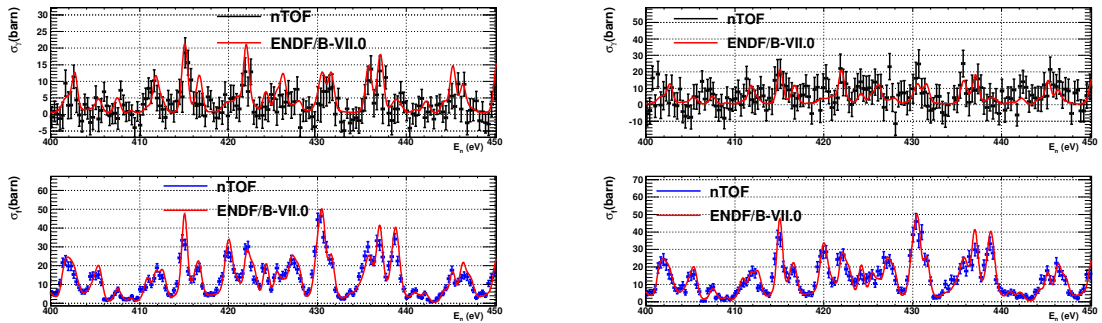


Fig. 8: Preliminary capture (top) and fission (bottom) cross sections obtained with the TAC and with the micro-megas, calculated from the 2 FTMGAS (left) and 10 FTMGAS (right) configurations, in the 400-450 eV energy range.

4 Future Work

We have presented a brief description of the experimental setup and a very preliminary analysis of the measured data. At this moment, a detailed and complete analysis of the measurement is being performed.

Acknowledgments

This work was supported by the European Commission within the Seventh Framework Programme through Fission-2010-ERINDA (project no.269499), the Spanish national company for radioactive waste management ENRESA, through the CIEMAT ENRESA agreements on "Transmutación de residuos radiactivos de alta actividad" the Spanish Plan Nacional de I+D+i de Física de Partículas (project FPA2008-04972-C03-01 and FPA2011-28770-C03-01), the Spanish Ministerio de Ciencia e Innovación through the CONSOLIDER CSD 2007-00042 project.

References

- [1] A.J. Koning *et al.*, CANDIDE: Nuclear data for sustainable nuclear energy EUR 23977 EN (2009).
- [2] Working Party on International Evaluation Co-operation of the NEA Nuclear Science Committee, Uncertainty and target accuracy assessment for innovative systems using recent covariance data evaluations, ISBN 978-92-64-99053-1 (2008).
- [3] NEA Nuclear Data High Priority Request List, <http://www.nea.fr/dbdata/hprl/index.html>.
- [4] C. Guerrero *et al.*, Eur. Phys. J. A (2013) 49
- [5] U. Abbondanno *et al.*, CERN n TOF Facility: Performance Report, CERN-SL-2002-053 ECT (2002).
- [6] C. Guerrero *et al.*, Nucl. Instr. Meth. A 608 (2009)
- [7] S. Andriamonje *et al.*, J. Korean Phys. Soc. 59 (2011).
- [8] U. Abbondanno *et al.*, Nucl. Inst. Meth A, 538 (2005) 692.
- [9] C. Guerrero *et al.*, Eur. Phys. J. A 48 (2012)
- [10] M. Jandel *et al.*, Phys. Rev. Lett. 109 (2012)
- [11] M.B. Chadwick *et al.*, Nuclear Data Sheets 107 (2006)